Spin pumping at the $Co_2FeAl_{0.5}Si_{0.5}$/Pt interface*

Wu Yong(吴 勇)[a], Zhao Yue-Lei(赵月雷)[a)b)], Xiong Qiang(熊 强)[a], Xu Xiao-Guang (徐晓光)[a)†], Sun Young(孙 阳)[b)], Zhang Shi-Qing(张十庆)[c)], and Jiang Yong(姜 勇)[a)]

[a)] *State Key Laboratory for Advanced Metals and Materials, School of Materials Science and Engineering, University of Science and Technology Beijing, Beijing* 100083, *China*

[b)] *Beijing National Laboratory for Condensed Matter Physics, Institute of Physics, Chinese Academy of Sciences, Beijing* 100190, *China*

[c)] *Chongqing Materials Research Institute, Chongqing* 400700, *China*

(Received 29 March 2013; revised manuscript received 9 May 2013; published 3 December 2013)

Spin pumping at the $Co_2FeAl_{0.5}Si_{0.5}$/Pt and Pt/$Co_2FeAl_{0.5}Si_{0.5}$ interfaces has been studied by ferromagnetic resonance technology (FMR). The spin mixing conductance of the $Co_2FeAl_{0.5}Si_{0.5}$/Pt and Pt/$Co_2FeAl_{0.5}Si_{0.5}$ interfaces was determined to be 3.7×10^{19} m^{-2} and 2.1×10^{19} m^{-2} by comparing the Gilbert damping in a $Co_2FeAl_{0.5}Si_{0.5}$ single film, $Co_2FeAl_{0.5}Si_{0.5}$/Pt bilayer film and a Pt/$Co_2FeAl_{0.5}Si_{0.5}$/Pt trilayer film. Spin pumping is more efficient in the $Co_2FeAl_{0.5}Si_{0.5}$/Pt bilayer film than in permalloy/Pt bilayer film.

Keywords: spin pumping, spin mix conductance, Gilbert damping constant, $Co_2FeAl_{0.5}Si_{0.5}$

PACS: 85.75.–d, 07.57.Pt, 46.40.Ff **DOI:** 10.1088/1674-1056/23/1/018503

1. Introduction

With the rapid development of spintronics, the manipulation of spin current is becoming crucial to the realization of efficient spin-based magnetic memories and logic devices.[1,2] Pure spin currents can be created by many methods, such as spin injection from ferromagnets,[3–6] the spin Hall effect,[7,8] spin pumping,[9–12] or the spin Seebeck effect.[13,14] Spin pumping, in particular, which is the emission of a pure spin current induced by magnetization dynamics (as shown in Fig. 1(a)), attracts a great deal of attention because it does not depend on elaborate nanoscale devices.

Most of the experience with spin pumping comes from combining it with an inverse spin Hall effect (ISHE) to generate or detect spin current in ferromagnetic metal (FM)/normal metal (NM) bilayers.[8] Recently, it has been investigated in terms of the Gilbert damping enhancement at FM/NM interfaces,[11,12] because the spin current generated from spin pumping exerts additional torque on the processing magnetizations, which effectively enhances the Gilbert damping at the FM/NM interface. The Gilbert damping constant is obtained by measuring and fitting ferromagnetic resonance (FMR) spectroscopy according to classic FMR theory.[15] The spin mixing conductance $g_{\uparrow\downarrow}$ at the FM/NM or NM/FM interface determines the efficiency of spin pumping, which can be calculated by the enhancement of the Gilbert damping.[16]

Cobalt-based Heusler alloys (Co_2MnSi, Co_2FeSi, and $Co_2FeAl_{0.5}Si_{0.5}$, etc.), due to their high spin polarization, have attracted great interest and are widely used in spintronic devices such as magnetic tunnel junctions[17–19] and spin valves.[20] However, very few studies have addressed the spin pumping effect at the interface of Heusler alloy films and Pt. In 2011, Chudo *et al.* studied the spin pumping efficiency of Co_2MnSi/Pt, Co_2FeSi/Pt and Co_2FeAl/Pt bilayers by FMR and ISHE, finding large spin mixing conductance comparable to that of permalloy (Py)/Pt ($g_{\uparrow\downarrow} = 2.6\times10^{19}$ m^{-2}).[21,22] Theoretical calculations show that the spin polarization of $Co_2FeAl_{0.5}Si_{0.5}$ (CFAS) has superior thermal stability[23] compared to other Co-based Heusler alloys. However, no study of the spin pumping efficiency of CFAS/Pt or Pt/CFAS interfaces has been reported. The present paper details our investigation of the spin pumping efficiency of CFAS/Pt and Pt/CFAS interfaces for thin CFAS films. The spin mixing conductance at the CFAS/Pt and Pt/CFAS interfaces has been calculated by comparing the calculations of Gilbert damping for the CFAS single layer, the CFAS/Pt bilayer and the Pt/CFAS/Pt trilayer.

2. Experiments

The films were prepared by magnetron sputtering under 0.7 Pa of Ar on Si(100)/SiO_2 substrates. The base pressure was lower than 8.0×10^{-6} Pa. We fabricated three different structures: CFAS (3), CFAS (3)/Pt (5), and Pt (10)/CFAS (3)/Pt (5), with the numbers indicating film thickness in nanometers. Magnetic measurements were performed on an alternating gradient magnetometer (AGM) at room temperature. The ferromagnetic resonance (FMR) measurements were carried out using a JEOL JES-FA200 ESR spectrometer at X-

*Project supported by the National Basic Research Program of China (Grant No. 2012CB932702), the National Natural Science Foundation of China (Grant Nos. 51271020, 51071022, and 11174031), the Program for Changjiang Scholars and Innovative Research Team in University, China (PCSIRT), the Beijing Nova Program, China (Grant No. 2011031), and the Fundamental Research Funds for the Central Universities of Ministry of Education of China.

†Corresponding author. E-mail: xgxu@ustb.edu.cn

© 2014 Chinese Physical Society and IOP Publishing Ltd

band frequencies (9.0 GHz) at room temperature. A schematic of the apparatus is shown in Fig. 1(b). The sample was fixed on a quartz rod to measure the out-of-plane (the field rotated with respect to film normal) angular dependence of the resonance field and the linewidth of the FMR spectra.[24] Figure 1(c) shows the coordinate system of samples for analysis and measurements. The symbols $\boldsymbol{M}$, $\boldsymbol{H}$, and $\boldsymbol{h}$ indicate the vectors of magnetization, the external direct current magnetic field, and the external microwave field, respectively. Here, $\boldsymbol{H}$ is rotated in the x–y plane ($\varphi_{\boldsymbol{A}} = \varphi_{\boldsymbol{H}} = 0$).

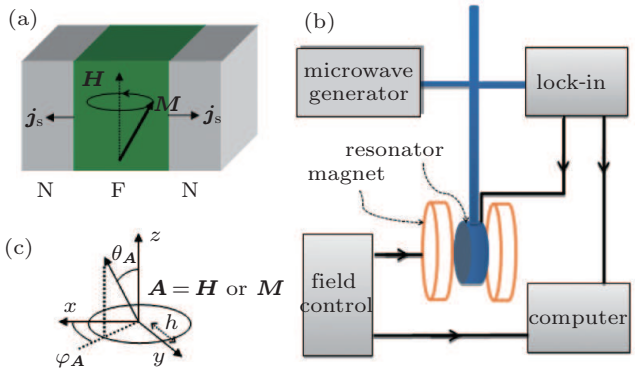


Fig. 1. (color online) (a) Schematic of spin pumping in a trilayer system, $\boldsymbol{H}$, $\boldsymbol{M}$, $\boldsymbol{j}_s$, F, and N denote the external magnetic field, processing magnetization of the ferromagnetic layer, spin current generated by the spin pumping, ferromagnetic layer, and normal metal layer, respectively. (b) Schematic of the apparatus used in the experiment. The sample was fixed on a quartz rod then placed in the resonant cavity to measure the FMR signal. (c) Coordinate system used for measurement and analysis of the out-of-plane angular dependence of FMR.

3. Results and discussion

Figure 2 shows the field swept FMR spectra measured for the CFAS (3) monolayer, CFAS (3)/Pt (5) bilayer and Pt (10)/CFAS (3)/Pt (5) trilayer, respectively. All the spectra have the typical Lorentzian line shape, but the linewidth of the Pt/CFAS/Pt trilayer is much wider than that of the CFAS/Pt bilayer due to the additional Pt/CFAS interface. A similar contrast can be observed between the CFAS/Pt bilayer and the single CFAS film. The broadened spectral widths mean that the relaxation of uniform magnetization precession is enhanced by the spin pumping that occurs at the interface between the Pt and the CFAS films, since the spin pumping can be regarded as a Gilbert-like damping and the spectral widths are proportional to the Gilbert damping constant, ignoring any inhomogeneous contribution to linewidth. A notable inhomogeneous contribution can result from disorder in the samples. This disorder includes variable magnetic properties and spin wave excitations. In our samples, the spin wave mode is not observed and after theoretical fitting, the variability of magnetization's contribution to linewidth is nearly negligible when the magnetic field is parallel to films.

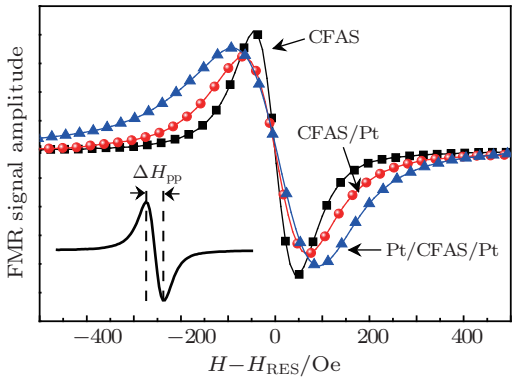


Fig. 2. (color online) Magnetic field dependence of the FMR signals for the CFAS (3) film, CFAS (3)/Pt (5) bilayer and Pt (10)/CFAS (3)/Pt (5) trilayer, respectively, ΔH_{pp} is the linewidth of the FMR spectra defined in the inset.

In order to evaluate the efficiency of spin pumping at CFAS/Pt and Pt/CFAS interfaces, we measured and analyzed the angular dependence of FMR spectra. Figures 3(a) and 3(b) show typical measurements of the out-of-plane angular (θ_H) dependence of the resonance field (H_{RES}) and linewidth (ΔH_{pp}), respectively, for the CFAS (3) film. The H_{RES} increases as θ_H decreases due to the enlarged demagnetization field in the out-of-plane direction. At intermediate angles, ΔH_{pp} shows a sharp peak, because the easy axis of magnetization lies in the plane of the sample; when the magnetic field $\boldsymbol{H}$ is rotated out of the plane, the magnetization $\boldsymbol{M}$ falls behind $\boldsymbol{H}$. The maximum separation of $\boldsymbol{M}$ and $\boldsymbol{H}$ occurs at a certain angle, which results in the maximum relaxation of uniform magnetization precession. According to the theory of FMR for an out-of-plane applied field, the resonance field is obtained from the dispersion equation given by

$$\omega/\gamma = \sqrt{H_1 \times H_2}, \tag{1}$$

$$H_1 = H_{RES}\cos(\theta_H - \theta_M) - 4\pi M_{eff}\cos^2\theta, \tag{2}$$

$$H_2 = H_{RES}\cos(\theta_H - \theta_M) - 4\pi M_{eff}\cos 2\theta. \tag{3}$$

Here, ω and γ are the resonance frequency and the gyromagnetic ratio, respectively, γ is given by $\gamma = g\mu_B/\hbar$, where g, μ_B, and $\hbar$ are the g-factor, the Bohr magneton and the Planck constant, respectively, M_{eff} is the effective magnetization, defined as $M_{eff} = M_S - K_\perp/2\pi M_S$, where $K_\perp$ is the perpendicular anisotropy energy density. The theoretical linewidth is expressed as[24]

$$\Delta H_{pp} = \Delta H_{pp}^{\alpha} + \Delta H_{pp}^{4\pi M_{eff}} + \Delta H_{pp}^{\Delta\theta_H}, \tag{4}$$

$$\Delta H_{pp}^{\alpha} = \frac{1}{\sqrt{3}}\left[\alpha(H_1 + H_2)\left|\frac{d(\omega/\gamma)}{dH_{RES}}\right|^{-1}\right], \tag{5}$$

$$\Delta H_{pp}^{4\pi M_{eff}} = \frac{1}{\sqrt{3}}\left|\frac{dH_{RES}}{d(4\pi M_{eff})}\right|\Delta(4\pi M_{eff}), \tag{6}$$

$$\Delta H_{pp}^{\Delta\theta_H} = \frac{1}{\sqrt{3}}\left|\frac{dH_{RES}}{d(\theta_H)}\right|\Delta\theta_H. \tag{7}$$

Here, ΔH_{pp}^{α} is the contribution of the Gilbert damping to the linewidth, $\Delta H_{pp}^{4\pi M_{eff}}$ and $\Delta H_{pp}^{\Delta\theta_H}$ represent the inhomogeneous

contributions arising from variations of the effective demagnetization field's magnitude and direction, respectively. We fitted our experimental results of the angular dependencies of H_{RES} and ΔH_{PP} using Eqs. (1)–(7). The results are shown in Figs. 3(a) and 3(b). The fitting damping constant is 0.024 for the CFAS (3) single film, which is bigger than the previously reported values for as-deposited Co_2FeSi (~ 0.008)[25] and Co_2FeAl (~ 0.005)[26] due to the film's thickness and non-epitaxial growth. From the fitting results in Fig. 3(b), we find that the origin of the linewidth is mainly attributable to the Gilbert damping for the CFAS (3) film and that the disorder's inhomogeneous contribution to the linewidth is almost negligible.

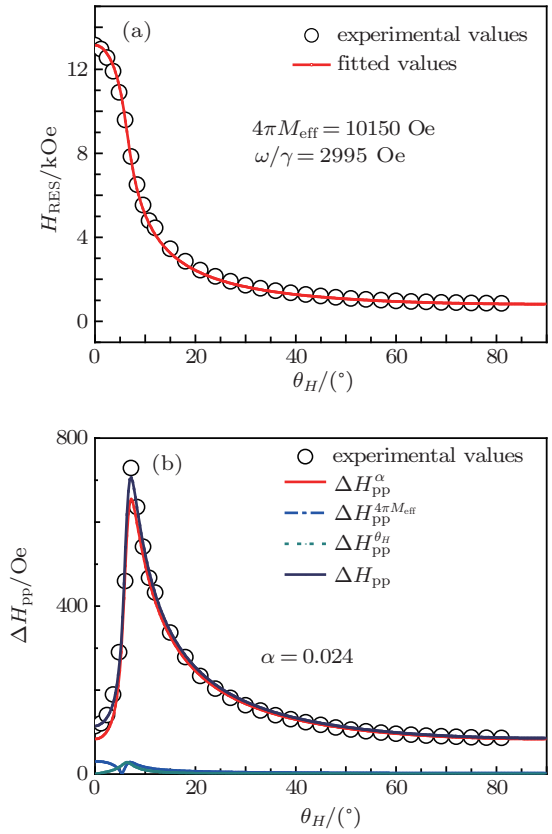


Fig. 3. (color online) Angular dependence of the (a) resonance field and (b) linewidth for the CFAS (3) single film. Open circles represent the experimental data. Bold lines indicate the calculated values. Thin, dash-dot and dotted lines represent the three components of the total linewidth, respectively: Gilbert damping (α), fluctuation of θ_H ($\Delta\theta_H$) and distribution of effective demagnetization ($\Delta(4\pi M_{eff})$).

Figures 4(a) and 4(b) show the θ_H-dependencies of H_{RES} and ΔH_{PP}, respectively, in the CFAS (3)/Pt (5) bilayer. The α value of the CFAS (3)/Pt (5) film is 0.037, which is bigger than that of the CFAS (3) single film due to the spin pumping at the interface of CFAS and the Pt capping layer. The spin-pumping enhanced damping of the capping layer can be calculated as $\Delta\alpha_{sp}^{cap} = 0.013$. Figures 5(a) and 5(b) show the θ_H dependence of H_{RES} and ΔH_{PP}, respectively, in the Pt (10)/CFAS (3)/Pt (5) trilayer. Its ΔH_{PP} is notably bigger than that of the CFAS (3)/Pt (5) film. The fitting results indicate that in the trilayer, the disorder's inhomogeneous contribution to linewidth is also significantly larger. One possible reason is that the morphologies of CFAS on SiO_2 and Pt differ. The Pt/CFAS interface is rougher than the SiO_2/CFAS interface. The α value of the Pt (10)/CFAS (3)/Pt (5) film is 0.047, which is bigger than that of the CFAS (3)/Pt (5) bilayer. This is reasonable, because the bilayer has only one interface where spin pumping occurs, while the trilayer has two. We also deposited of Pt (10)/CFAS (t)/Pt (5) structures with different CFAS and calculated the corresponding damping values. Detailed parameters are shown in Table 1. As expected, α decreases remarkably with the increasing thickness of CFAS, in good agreement with a previous report for Pt/Py/Pt films with a thin Py layer, suggesting that interfacial spin pumping contributes significantly to damping.[24,26] By these comparative experiments, we can separate the contributions of the seed and capping layers for a fixed thickness ($t = 3$ nm) of CFAS ($\Delta\alpha_{sp}^{seed} = 0.01$).

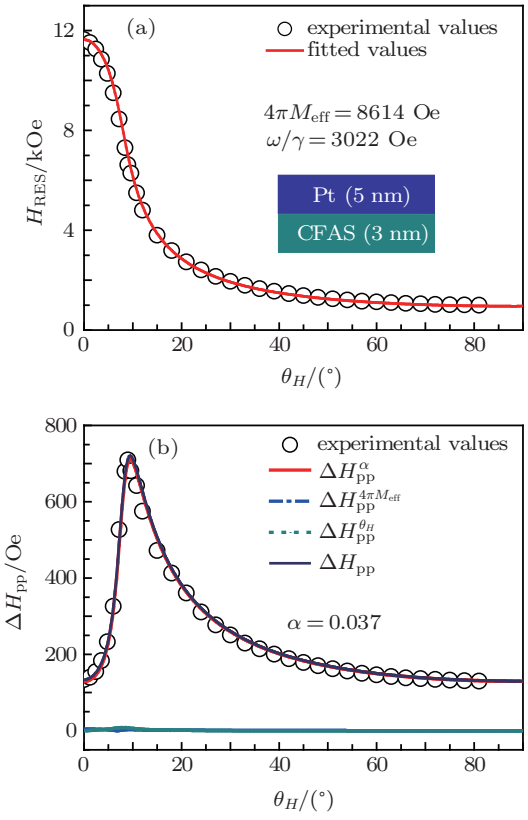


Fig. 4. (color online) Angular dependence of resonance field H_{RES} (a) and linewidth ΔH_{pp} (b) for the CFAS (3)/Pt (5) bilayer.

The enhancement of damping by spin pumping is described by[16]

$$\Delta\alpha_{sp}^{cap(seed)} = g\mu_B \frac{g_{\uparrow\downarrow}}{4\pi M_S} \frac{1}{t_{CFAS}} (1 - e^{-2t_{Pt}/\lambda_{Pt}}), \qquad (8)$$

where λ_{Pt} denotes the spin diffusion length of the Pt layer ($\lambda_{Pt} = 10$ nm[21]), M_S is the saturation magnetization, t_{CFAS}

and t_{Pt} are the thicknesses of CFAS and Pt, respectively. Using Eq. (8) with $M_S = 923.43$ emu/cm^3, the spin mixing conductance $g_{\uparrow\downarrow}$ is calculated to be 3.7×10^{19} m^{-2} at the CFAS/Pt interface and 2.1×10^{19} m^{-2} at the Pt/CFAS interface. Interestingly, the CFAS/Pt and Pt/CFAS interfaces have different spin mixing conductances, because the diffusive spin current in the Pt layer has a different probability of diffusing back to the CFAS/Pt or Pt/CFAS interface before depolarization. Moreover, our results show that spin pumping is more efficient in the CFAS/Pt bilayer film than in the Py/Pt bilayer film. This means that the CFAS/Pt interface has a higher spin polarization than the Py/Pt interface.

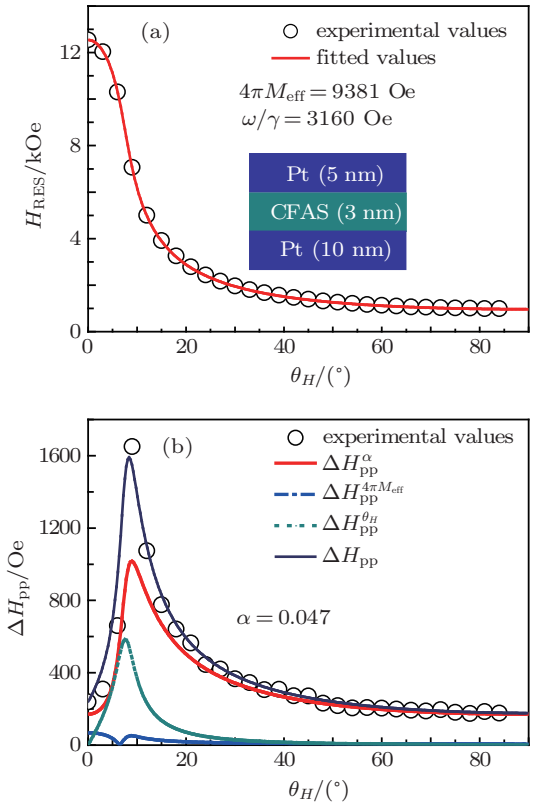


Fig. 5. (color online) Angular dependence of resonance field H_{RES} (a) and linewidth ΔH_{pp} (b) for Pt (10)/CFAS (3)/Pt (5) trilayer.

Table 1. Fitting parameters for the samples Pt (10)/CFAS (t)/Pt (5).

t_{CFAS}/nm	M_{eff}/Oe	$\Delta(4\pi M_{eff})$/Oe	$\Delta(\theta_H)$/(°)	g	α
2.5	696	319	0.95	2.003	0.055
3.0	7474	117	0.85	2.032	0.047
3.5	728	137	0.88	2.045	0.035
4.0	773	62	0.58	2.037	0.030

4. Summary

We have investigated spin pumping efficiency at the CFAS/Pt and Pt/CFAS interfaces in terms of the Gilbert damping enhancement measured by FMR. The spin mixing conductance at the CFAS/Pt and Pt/CFAS interfaces arecalculated to be 3.7×10^{19} m^{-2} and 2.1×10^{19} m^{-2}, respectively. Spin pumping is more efficient in the CFAS/Pt bilayer film than in the Py/Pt bilayer film.

References

[1] Zutic I, Fabian J and Sarma S D 2004 *Rev. Mod. Phys.* **76** 323
[2] Maekawa E 2006 *Concept in Spin Electronics* (Oxford: Oxford University)
[3] Jedema F J, Filip A T and van Wees B J 2001 *Nature* **410** 345
[4] Takahashi S and Maekawa 2003 *Phys. Rev. B* **67** 052409
[5] Fukuma Y, Wang L, Idzuchi H, Takahashi S and Maekawa S 2011 *Nat. Mater.* **10** 527
[6] Yuan S P, Shen C, Zheng H Z, Liu Q, Wang L G, Meng K K and Zhao J H 2013 *Chin. Phys. B* **22** 047202
[7] Hirsch J E 1999 *Phys. Rev. Lett.* **83** 1834
[8] Brüne C, Roth A, Novik E G, König M, Buhmann H, Hankiewicz E M, Hanke W, Sinova J and Molenkamp L W 2010 *Nat. Phys.* **6** 448
[9] Nakayama H, Ando K, Harii K, Kajiwara Y, Yoshino T, Uchida K and Saitoh E 2010 *IEEE Trans. Magn.* **46** 2202
[10] Heinrich B, Burrowes C, Montoya E, Kardasz B, Girt E, Song Y Y, Sun Y Y and Wu M Z 2011 *Phys. Rev. Lett.* **107** 066604
[11] Charilaou M, Lenz K and Kuch W 2010 *J. Magn. Magn. Mater.* **322** 2065
[12] Shaw J M, Nembach H T and Silva T J 2012 *Phys. Rev. B* **85** 054412
[13] Uchida K, Ota T, Harii K, Takahashi S, Maekawa S, Fujikawa Y and Saitoh E 2010 *Solid State Commun.* **150** 524
[14] Bosu S, Sakuraba Y, Uchida K, Saito K, Ota T, Saitoh E and Takanashi K 2011 *Phys. Rev. B* **83** 224401
[15] Vonsovskii S V 1996 *Ferromagnetic Resonance* (Oxford: Pergamon Press)
[16] Foros J, Woltersdorf G, Heinrich B and Brataas A 2005 *J. Appl. Phys.* **97** 10A714
[17] Tezuka N, Ikeda N, Mitsuhashi F and Sugimoto S 2008 *Appl. Phys. Lett.* **94** 162504
[18] Li X Q, Xu X G, Wang S, Wu Y, Zhang D L, Miao J and Jiang Y 2012 *Chin. Phys. B* **21** 107307
[19] Wang S, Li X Q, Bai L J, Xu X G, Miao J and Jiang Y 2013 *Chin. Phys. B* **22** 057305
[20] Sato J, Oogane M, Naganuma H and Ando Y 2011 *Appl. Phys. Express* **4** 113005
[21] Chudo H, Ando K, Saito K, Okayasu S, Haruki R, Sakuraba Y, Yasuoka H, Takanashi K and Saitoh E 2011 *J. Appl. Phys.* **109** 073915
[22] Czeschka F D, Dreher L, Brandt M S, Weiler M, Althammer M, Imort I-M, Reiss G, Thomas A, Schoch W, Limmer W, Huebl H, Gross R and Goennenwein S T B 2011 *Phys. Rev. Lett.* **107** 046601
[23] Fecher G H and Felser C 2007 *J. Phys. D: Appl. Phys.* **40** 1582
[24] Mizukami S, Ando Y and Miyazaki T 2001 *Jpn. J. Appl. Phys.* **40** 580
[25] Oogane M, Yilgin R, Shinano M, Yakata S, Sakuraba Y, Ando Y and Miyazaki T 2007 *J. Appl. Phys.* **101** 09J501
[26] Mizukami S, Watanabe D, Oogane M, Ando Y, Miura Y, Shirai M and Miyazaki T 2009 *J. Appl. Phys.* **105** 07D306